Published in final edited form as:
J Control Release. 2011 December 20; 156(3): 276–280. doi:10.1016/j.jconrel.2011.08.019.

Photoactivation Switch from Type II to Type I Reactions by Electron-Rich Micelles for Improved Photodynamic Therapy of Cancer Cells Under Hypoxia

Huiying Ding[a], **Haijun Yu**[a], **Ying Dong**[a], **Ruhai Tian**[a], **Gang Huang**[a], **David A. Boothman**[a], **Baran D. Sumer**[b], and **Jinming Gao**[*,a]

[a]Department of Pharmacology, Harold C. Simmons Comprehensive Cancer Center, University of Texas Southwestern Medical Center at Dallas, 5323 Harry Hines Boulevard, Dallas, Texas 75390

[b]Department of Otolaryngology, Head and Neck Surgery, University of Texas Southwestern Medical Center at Dallas, 5323 Harry Hines Boulevard, Dallas, Texas 75390

Abstract

Photodynamic therapy (PDT) is an emerging clinical modality for the treatment of a variety of diseases. Most photosensitizers are hydrophobic and poorly soluble in water. Many new nanoplatforms have been successfully established to improve the delivery efficiency of PS drugs. However, few reported studies have investigated how the carrier microenvironment may affect the photophysical properties of PS drugs and subsequently, their biological efficacy in killing malignant cells. In this study, we describe the modulation of type I and II photoactivation processes of the photosensitizer, 5,10,15,20-tetrakis(*meso*-hydroxyphenyl)porphyrin (mTHPP), by the micelle core environment. Electron-rich poly(2-(diisopropylamino)ethyl methacrylate) (PDPA) micelles increased photoactivations from type II to type I mechanisms, which significantly increased the generation of $O_2^{\bullet -}$ through the electron transfer pathway over $^1O_2$ production through energy transfer process. The PDPA micelles led to enhanced phototoxicity over the electron-deficient poly(D,L-lactide) control in multiple cancer cell lines under argon-saturated conditions. These data suggest that micelle carriers may not only improve the bioavailability of photosensitizer drugs, but also modulate photophysical properties for improved PDT efficacy.

Keywords

Photodynamic therapy; polymeric micelles; nanoparticle delivery; photoinduced electron transfer; reactive oxygen species

Concept and Hypothesis

Photodynamic therapy (PDT) is an emerging clinical modality that has received considerable attention for the treatment of cancer, cardiovascular, dermatological, and ophthalmic diseases [1–3]. PDT has three essential elements: a photosensitizer (PS), light

[*]Address correspondence to jinming.gao@utsouthwestern.edu.

Supporting Information Available: Materials, characterization of polymers by ^{1}HNMR and GPC, UV-Vis and fluorescence spectra of mTHPP, confocal laser scanning microscopy images of PC-3 cells, the phototoxicity of free mTHPP, intracellular mTHPP accumulation kinetics in H2009 cells, phototoxicity of the mTHPP-loaded micelle at dose of 150 μg/ml.

and oxygen. New photosensitizing drugs based on porphyrins and chemically related compounds such as chlorins and phthalocyanines have been under extensive investigations [4, 5]. Most photosensitizers are hydrophobic and poorly soluble in water. A variety of nanoplatforms (e.g. polymer conjugates [6], polymeric micelles [7, 8], liposomes [9], ceramic nanoparticles [10]) have been successfully established to improve drug availability for parenteral administration, and to further increase nanoparticle uptake (e.g. through the leaky tumor vasculature) for enhanced therapeutic efficacy. Despite these exciting advances, few reported studies have been focused on the carrier-drug interactions, and in particular, how the carrier microenvironment may affect the photophysical properties of PS drugs, and subsequently, their biological efficacy in killing malignant cells.

Upon light activation, an excited photosensitizer can undergo type I (electron transfer) and/or type II (engery transfer) reactions to produce highly reactive oxygen species (ROS), resulting in necrosis and/or apoptosis of exposed cells [11–13]. Type I reactions generate radical and radical anion species (e.g., $O_2^{\bullet -}$, $HO^{\bullet}$), while type II reactions produce singlet oxygen ($^1O_2$). For the Type II pathway, PDT effect is highly dependent on the oxygen content. In cancer therapy, the inner region of a tumor is commonly hypoxic (<20 mmHg O_2 pressure) [14] due to insufficient blood supply. In addition, oxygen shortages can occur as a result of photochemical consumption and vascular damage during PDT, which further limits the efficacy in tumor destructions [15]. The type I mechanism involves hydrogen-atom abstraction or electron-transfer between the excited PS and a substrate, yielding free radicals [16]. These two competing mechanisms can occur simultaneously [17]. It is generally believed that $^1O_2$ formed from a type II reaction is primarily responsible for the biological PDT effect [18, 19], however, several recent studies indicate that radical species from the type I mechanism may lead to an amplified PDT response, particularly under low oxygen conditions [20, 21]. Direct comparisons between the contributions of type I and type II mechanisms to PDT efficacy are difficult due to the complexity of ROS formation on environmental factors.

In a previous study, we reported that polymeric micelles provided a favorable microenvironment rendering enhanced properties of the incorporated PS, such as the increased water solubility and stability, decreased aggregation, brighter fluorescence emission, and improved PDT efficacy *in vitro* [22]. In this paper, we describe the modulation of the type I and II photoreactions from a model PS agent (Scheme 1), 5,10,15,20-tetrakis(*meso*-hydroxyphenyl) porphyrin (mTHPP) by carrier-drug interactions. We hypothesize that the electron-rich micelle core can serve as an electron reservoir to preferentially promote type I reactions for PDT, despite using a type II PS agent (Scheme 1). Encapsulation of mTHPP in the core of electron-rich poly(ethylene glycol)-*b*-poly(2-(diisopropylamino)ethyl methacrylate (PEG-*b*-PDPA) micelles dramatically increased the production of type I radical species over the electron-deficient PEG-*b*-poly(D,L-lactide) (PEG-*b*-PLA) micelle control. The increase in type I mechanism led to increased production of anion radicals, and significantly improved PDT efficacy in killing several types of cancer cells under hypoxic conditions. This quantifiable difference in efficacy helped to clarify the relative contributions of $^1O_2$ and $O_2^{\bullet -}$ to the PDT effect, elucidating the mechanism of action of a clinical treatment modality.

Experimental Methods

Preparation of mTHPP-loaded micelles

PEG-*b*-PDPA and PEG-*b*-PLA copolymers were synthesized using atom transfer radical polymerization (ATRP) [23] and ring-opening polymerization [24] methods, respectively. The PEG segments in both copolymers were controlled at 5 kD. The PDPA and PLA segments were controlled at 10 kD. mTHPP-loaded PEG-*b*-PLA (mTHPP-PLA) and PEG-*b*-

PDPA (mTHPP-PDPA) micelles were produced using a solvent evaporation method [25]. Briefly, a proper amount of the copolymer was first dissolved in tetrahydrofuran (THF) with an mTHPP weight ratio of 2%. The mixture was added dropwise to MilliQ water under sonication and then allowed to evaporate overnight to remove THF. The resulting mTHPP-loaded micelles were purified by centrifugation dialysis (MW cutoff 100KD) to remove free mTHPP and polymer.

Micelle characterizations

The mTHPP micelles were characterized by transmission electron microscopy (TEM, JEOL 1200EX II model) for particle morphology and zeta sizer (Malvern NanoZS) for zeta potential and hydrodynamic diameters. The mTHPP loading density was measured by dissolving a solid micelle sample in THF and quantified by UV-Vis analysis using a previously established calibration curve. The UV-Vis absorption spectra of mTHPP micelles were recorded at room temperature using a Shimadzu UV spectrophotometer (UV-1800), the emission spectra were obtained using a Hitachi fluorescence spectrophotometer (F-7000 model). The fluorescence quantum yields (Φ_F) of mTHPP micelles were calculated by comparison of the area below the emission spectra with free mTHPP ($\Phi_F = 0.12$ [26]). Electrochemical measurements were performed using a Princeton applied Research/EG&G Model 283 potentiostat and a standard three-electrode cell outfitted with a Pt counter electrode and a saturated calomel electrode (SCE) reference electrode at a scan rate of 100 mV/S. The results were shown in Table 1. Singlet oxygen generation was measured by electron spin resonance (ESR) spectrum using 2,2,6,6-tetramethyl-4-piperodone (TEMP) as a spin trap [27] and quantified by the net loss of anthracene-9,10-dipropionic acid (ADPA) [28] absorption over time. Confocal imaging studies were performed on a Nikon TE2000E confocal laser scanning microscope (see details in the Supporting Information).

Detection of $^1O_2$ and $O_2^{\bullet-}$ by ESR

The ESR spectra were recorded at 25 °C on a Bruker ESP-300E spectrometer at 9.8 GHz, X-band with 100Hz field modulation. The samples were illuminated directly in the cavity of the ESR spectrometer with a Nd:YAG laser (532 nm, 5–6 ns pulse width, 10 Hz repetition frequency, 10 mJ pulse energy). The mTHPP-loaded micelle (200 μg/ml) solution in MilliQ water containing TEMP was irradiated. The produced $^1O_2$ reacted with TEMP to yield TEMPO, which was identified as a typical three-line ESR spectrum. mTHPP-PLA showed stronger ESR signals than mTHPP-PDPA at the same experimental conditions. Control experiments confirmed that oxygen, mTHPP, and light were all necessary to produce the ESR spectrum. The addition of scavenger, such as NaN_3, dramatically reduced the ESR signals.

When an air-saturated DMSO solution containing mTHPP (4 μg/ml) and copolymer (200 μg/ml) and DMPO (50 mM) was irradiated, a representative spectrum of DMPO-$O_2^{\bullet-}$ adduct was immediately observed. The hyperfine coupling constants and the positions were in good agreement with the literatures [29]. No signal was observed without light irradiations. The mTHPP-PDPA micelles showed approximately 3-fold increase in ESR signals over mTHPP-PLA micelles at the same conditions. By adding superoxide dismutase (SOD), an efficient scavenger of $O_2^{\bullet-}$, the ESR signal was suppressed, which further confirmed the assignment of the ESR spectra to DMPO-$O_2^{\bullet-}$ adduct.

Detection of $O_2^{\bullet-}$ by DHE in cancer cells *in vitro*

H2009 lung cancer and PC-3 prostate cancer cells were cultured in RPMI 1640 medium supplemented with 5% fetal bovine serum and antibiotics (Penicillin-Streptomycin) at 37 °C in a 10% CO_2 humidified incubator. Cells were seeded in a glass-bottomed culture dish and allowed to attach overnight. The media were replaced with fresh media containing 150 μg/

mL mTHPP-loaded micelles for 2 hrs, followed by incubation with DHE for 30 mins in air or argon-saturated PBS, then irradiated with 532 nm laser light at 20 mw/cm^2 for 4 mins. The cells were examined under 60× magnification (λ_{ex} = 543 nm, λ_{em} = 605 ± 35 nm). ImageJ software (National Institutes of Health) was utilized to quantify the mean fluorescence intensity (MFI) of the oxidized DHE *in vitro*.

PDT efficacy of mTHPP-loaded micelles

A549 lung cancer cells were cultured in DMEM medium supplemented with 5% fetal bovine serum and antibiotics (Penicillin-Streptomycin) at 37 °C in a 10% CO_2 humidified incubator. One day before PDT treatment, cells were trypsinized using 0.05% trypsin-EDTA and seeded (10,000 cells/well) into 96-well plates. Cell culture media were then replaced by media containing 150 or 200 g/ml doses of mTHPP micelles and incubated for 2 hrs. For the PDT study, plates were transferred to a hypoxia chamber under either an air or argon atmosphere, and illuminated with a laser (λ = 532 nm, power density = 20 mW/cm^2) for 10 mins. After irradiation, cells were allowed to grow for an additional 2 days in fresh media. Relative cell survival was measured by 3-[4,5-dimethylthiazol-2-yl]2,5-diphenyl tetrazolium bromide (MTT) spectrophotometric method [30] and data were graphed as means of treated/control (T/C) ± SD (standard deviation). Dark cytotoxicity was assessed from cells incubated with mTHPP-loaded micelles without laser light exposure.

Discovery and Interpretation

mTHPP-loaded micelles were produced by a solvent evaporation method. mTHPP loadings were controlled at 1.8 ± 0.5 and 1.9 ± 0.4 wt % for mTHPP-PLA and mTHPP-PDPA micelles, respectively. The hydrodynamic diameters were 49 ± 6 and 57 ± 6 nm for the two micelle formulations, respectively, by dynamic light scattering measurements. Micelles were spherical in shape by transmission electron microscopy analysis (Fig. 1, Table 1).

Free mTHPP molecules readily aggregated in aqueous solution with a broadened, red-shifted Soret band centered at 428 nm, resulting in loss of photochemical activity (Fig. S1). However, in polar solvents (e.g. methanol) or when encapsulated into micelles, mTHPP molecules stayed mostly monomeric as indicated by the sharp Soret band at 415–420 nm (Fig. 2A). Free mTHPP had a weak emission in aqueous solution (Φ_F < 0.01, Fig. S1). In contrast, both mTHPP micelles had about 10-fold increase in fluorescence quantum yields (Φ_F = 0.11 and 0.08 for mTHPP-PLA and mTHPP-PDPA mcielles, respectively), close to that of mTHPP in methanol (Φ_F = 0.12 [26]).

Micelles composed of mTHPP-PDPA are less efficient $^1O_2$ generators with a relative $^1O_2$ quantum yield (Φ_Δ) of 0.46 normalized to that of mTHPP-PLA micelles (Fig. 2B and C) in an air-saturated aqueous solution. Attempts were also made to trap superoxide anion radical ($O_2^{\bullet-}$) by 5,5-dimethyl-1-pyrroline-N-oxide (DMPO). However, the signal of the DMPO-$O_2^{\bullet-}$ adduct was hardly detected in H_2O or other protic solvents at room temperature [31, 32]. Instead, we dissolved mTHPP and corresponding copolymers in DMSO, and measured their ESR signals after 532 nm light irradiation. A three-fold increase in $O_2^{\bullet-}$ generation was observed in the mTHPP-PEG-PDPA mixture compared to that of mTHPP-PEG-PLA (Fig. 2D). We hypothesize that the electron-rich amino moieties in the PDPA segment acted as electron donors and resulted in the formation of photoinduced charge separation states from excited triplet and/or singlet states of mTHPP that led to a higher yield of $O_2^{\bullet-}$ by the type I mechanism (Scheme 1). This was also supported by the decreased fluorescence intensity of mTHPP-PDPA compared to mTHPP-PLA micelles (Fig. 2A), which was probably due to photobleaching of mTHPP by the type I photochemical reaction. In the electron-deficient PLA environment, mTHPP underwent typical type II reactions, where $^1O_2$ was predominantly formed (Fig. 2B and C). The high $O_2^{\bullet-}$ and low $^1O_2$ changes in the

mTHPP-PDPA system can be attributed to the formation of an intermolecular charge transfer state. The electron transfer between amino moieties and the excited state of mTHPP is thermodynamically feasible. The free Gibbs energy (ΔG) was calculated as −35.6 kJ/mol from the simplified Rehm-Weller [33] equation ($\Delta G = E_{ox} - E_{red} - E_{0\text{-}0}$) by using the excited state energy of mTHPP ($E_{0\text{-}0}$ = 2.0 eV, which corresponds to the intersection point of the absorption and emission spectra), the oxidation potential of PEG-PDPA in acetonitrile (0.65 V vs. SCE) and the reduction potential of mTHPP in THF (−0.98 V vs. SCE) obtained from cyclic voltammetry, which were in accord with the published redox potentials [34, 35].

To evaluate the ROS formation in cancer cells under low oxygen concentrations, we used dihydroethidium (DHE) for $O_2^{\bullet-}$detection [36]. DHE can be oxidized by $O_2^{\bullet-}$ to 2-hydroxyethidium (2-OH-E^+) and ethidium (E^+) [37], which then intercalate into DNA and emit bright red fluorescence inside the cell nuclei. Fig. 3A shows confocal images of H2009 cells in air as well as argon-saturated RPMI 1640 medium 4 minutes post-irradiation with 532 nm laser light. The data show an approximately 3-fold increase in mean fluorescence intensity (MFI) in cells exposed to mTHPP-PDPA versus mTHPP-PLA micelles under argon conditions (Fig. 3B), supporting the hypothesis that mTHPP-PDPA was more efficient in producing ROS under hypoxic conditions. These data were further corroborated by similar results using PC-3 prostate cancer cells (Fig. S3).

The phototoxicity and dark toxicity of mTHPP-loaded micelles were examined in several human cancer cell lines (H2009 and A549 lung cancer cells, PC-3 prostate cancer cells, Fig. 4). Cells were incubated with 200 μg/ml mTHPP-loaded micelles for 2 hrs under air and argon atmospheres. For blank micelles without mTHPP, the cells did not show any observable phototoxicity or dark cytotoxicity (data not shown). The dark cytotoxicity of mTHPP-loaded PDPA or PLA micelles was minimal compared to control cells (Fig. 4). In the presence of air, mTHPP-PDPA and mTHPP-PLA micelles showed similar phototoxicity. The differences in baseline phototoxicity values between cell lines indicated the different sensitivities of cancer cells to ROS. In the absence of air, mTHPP-PDPA micelles showed significantly increased phototoxicity over the mTHPP-PLA micelles ($p < 0.01$) for all the tested cancer cell lines. For example, the relative survival of H2009 cells was 17.7 ± 2.5% for mTHPP-PDPA micelles, approximately 2-fold lower compared to mTHPP-PLA micelles (46.6 ± 4.1%, $p < 0.01$) and 3-fold lower compared to free mTHPP (62.8 ± 3.2%, $p < 0.01$) (Fig. S4). Comparison of phototoxicity of the two micelle groups at another dose (150 g/ml) showed a similar dependence (Fig. S5).

Conclusions

In summary, we report the development of a novel PS nanoparticle formulation that confers greater PDT cytotoxicity against cancer cells under hypoxic conditions. The photophysical and photodynamic properties of mTHPP are highly depdendent on the micelle core environment. With the electron-donating PDPA segment, the generation of $O_2^{\bullet-}$ through the electron transfer pathway competes with $^1O_2$ production through the energy transfer process under aerobic environments, and becomes dominant under hypoxic conditions. These data suggest that polymeric micelles can not only serve as important solubilization carriers for hydrophobic PS drugs, but also can be utilized to modulate type I and/or II reactions for efficacious ROS generation depending on the tumor microenvironment. Knowledge from this studies can lead to more effective PS systems (e.g. mTHPP-PDPA micelles) for the treatment of hypoxic tumors by PDT.

Acknowledgments

This research is supported by the National Cancer Institute to JG (R01CA122994 and R01CA129011) and to DAB (R01CA102792) and the National Center for Research Resources to BDS (5 UL1 RR024982-02). This is manuscript CSCN060 from the Program of Cell Stress and Cancer Nanomedicine in the Simmons Cancer Center. We thank Yanhong Liu at Technical Institute of Physics and Chemistry, CAS for assistance with ESR studies, and Vikram Kodibagkar and Praveen Gulaka for assistance on cell culture conditions under hypoxia.

References

1. Dougherty TJ, Gomer CJ, Henderson BW, Jori G, Kessel D, Korbelik M, Moan J, Peng Q. Photodynamic therapy. J Natl Cancer Inst. 1998; 90:889–905. [PubMed: 9637138]
2. Dolmans D, Fukumura D, Jain RK. Photodynamic therapy for cancer. Nat Rev Cancer. 2003; 3:380–387. [PubMed: 12724736]
3. Celli JP, Spring BQ, Rizvi I, Evans CL, Samkoe KS, Verma S, Pogue BW, Hasan T. Imaging and Photodynamic Therapy: Mechanisms, Monitoring, and Optimization. Chem Rev. 2010; 110:2795–2838. [PubMed: 20353192]
4. Moreira LM, dos Santos FV, Lyon JP, Maftoum-Costa M, Pacheco-Soares C, da Silva NS. Photodynamic therapy: Porphyrins and phthalocyanines as Photosensitizers. Aust J Chem. 2008; 61:741–754.
5. O'Connor AE, Gallagher WM, Byrne AT. Porphyrin and Nonporphyrin Photosensitizers in Oncology: Preclinical and Clinical Advances in Photodynamic Therapy. Photochem Photobiol. 2009; 85:1053–1074. [PubMed: 19682322]
6. Vaidya A, Sun YG, Feng Y, Emerson L, Jeong EK, Lu ZR. Contrast-Enhanced MRI-Guided Photodynamic Cancer Therapy with a Pegylated Bifunctional Polymer Conjugate. Pharm Res. 2008; 25:2002–2011. [PubMed: 18584312]
7. Roby A, Erdogan S, Torchilin VP. Enhanced in vivo antitumor efficacy of poorly soluble PDT agent, meso-tetraphenylporphine, in PEG-PE-based tumor-targeted immunomicelles. Cancer Biology & Therapy. 2007; 6:1136–1142. [PubMed: 17611407]
8. van Nostrum CF. Polymeric micelles to deliver photosensitizers for photodynamic therapy. Adv Drug Del Rev. 2004; 56:9–16.
9. Derycke ASL, de Witte PAM. Liposomes for photodynamic therapy. Adv Drug Del Rev. 2004; 56:17–30.
10. Roy I, Ohulchanskyy TY, Pudavar HE, Bergey EJ, Oseroff AR, Morgan J, Dougherty TJ, Prasad PN. Ceramic-based nanoparticles entrapping water-insoluble photosensitizing anticancer drugs: A novel drug-carrier system for photodynamic therapy. J Am Chem Soc. 2003; 125:7860–7865. [PubMed: 12823004]
11. Pass HI. Photodynamic Therapy in Oncology - Mechanisms and Clinical Use. J Natl Cancer Inst. 1993; 85:443–456. [PubMed: 8445672]
12. Castano AP, Mroz P, Hamblin MR. Photodynamic therapy and anti-tumour immunity. Nat Rev Cancer. 2006; 6:535–545. [PubMed: 16794636]
13. Juarranz Á, Jaén P, Sanz-Rodríguez F, Cuevas J, González S. Photodynamic therapy of cancer. Basic principles and applications. Clin Trans Onco. 2008; 10:148–154.
14. Moulder JE, Rockwell S. Tumor hypoxia: its impact on cancer therapy. Cancer Metastasis Rev. 1987; 5:313–341. [PubMed: 3552280]
15. Pogue BW, Braun RD, Lanzen JL, Erickson C, Dewhirst MW. Analysis of the heterogeneity of pO2 dynamics during photodynamic therapy with verteporfin. Photochem Photobiol. 2001; 74:700–706. [PubMed: 11723798]
16. Ochsner M. Photophysical and photobiological processes in the photodynamic therapy of tumours. J Photochem Photobiol B: Biol. 1997; 39:1–18.
17. Dougherty TJ, Gomer CJ, Henderson BW, Jori G, Kessel D, Korbelik M, Moan J, Peng Q. Photodynamic therapy. J Natl Cancer Inst. 1998; 90:889–905. [PubMed: 9637138]
18. Pineiro M, Gonsalves A, Pereira MM, Formosinho SJ, Arnaut LG. New halogenated phenylbacteriochlorins and their efficiency in singlet-oxygen sensitization. J Phys Chem A. 2002; 106:3787–3795.

19. Pineiro M, Pereira MM, Gonsalves A, Arnaut LG, Formosinho SJ. Singlet oxygen quantum yields from halogenated chlorins: potential new photodynamic therapy agents. Journal of Photochemistry and Photobiology a-Chemistry. 2001; 138:147–157.
20. Silva EFF, Serpa C, Dabrowski JM, Monteiro CJP, Formosinho SJ, Stochel G, Urbanska K, Simoes S, Pereira MM, Arnaut LG. Mechanisms of Singlet-Oxygen and Superoxide-Ion Generation by Porphyrins and Bacteriochlorins and their Implications in Photodynamic Therapy. Chem Eur J. 2010; 16:9273–9286. [PubMed: 20572171]
21. Vakrat-Haglili Y, Weiner L, Brumfeld V, Brandis A, Salomon Y, McIlroy B, Wilson BC, Pawlak A, Rozanowska M, Sarna T, Scherz A. The microenvironment effect on the generation of reactive oxygen species by Pd-bacteriopheophorbide. J Am Chem Soc. 2005; 127:6487–6497. [PubMed: 15853357]
22. Ding H, Sumer BD, Kessinger CW, Dong Y, Huang G, Boothman DA, Gao J. Nanoscopic micelle delivery improves the photophysical properties and efficacy of photodynamic therapy of protoporphyrin IX. J Control Release. 2011; 151:271–277. [PubMed: 21232562]
23. Massignani M, LoPresti C, Blanazs A, Madsen J, Armes SP, Lewis AL, Battaglia G. Controlling Cellular Uptake by Surface Chemistry, Size, and Surface Topology at the Nanoscale. Small. 2009; 5:2424–2432. [PubMed: 19634187]
24. Shuai X, Ai H, Nasongkla N, Kim S, Gao J. Micellar carriers based on block copolymers of poly(epsilon-caprolactone) and poly(ethylene glycol) for doxorubicin delivery. J Control Release. 2004; 98:415–426. [PubMed: 15312997]
25. Blanco E, Bey EA, Dong Y, Weinberg BD, Sutton DM, Boothman DA, Gao JM. beta-Lapachone-containing PEG-PLA polymer micelles as novel nanotherapeutics against NQO1-overexpres sing tumor cells. J Controlled Release. 2007; 122:365–374.
26. Bonnett R, Charlesworth P, Djelal BD, Foley S, McGarvey DJ, Truscott TG. Photophysical properties of 5,10,15,20-tetrakis(m-hydroxyphenyl)porphyrin-(m-THPP), 5,10,15,20-tetrakis(m-hydroxyphenyl)chlorin (m-THPC) and 5,10,15,20-tetrakis(m-hydroxyphenyl)bacteriochlorin (m-THPBC): a comparative study. J Chem Soc Perk T. 1999; 2:325–328.
27. Moan J, Wold E. Detection of singlet oxygen production by ESR. Nature. 1979; 279:450–451. [PubMed: 16068192]
28. Oar MA, Serin JA, Dichtel WR, Frechet JMJ. Photosensitization of singlet oxygen via two-photon-excited fluorescence resonance energy transfer in a water-soluble dendrimer. Chem Mater. 2005; 17:2267–2275.
29. Harbour JR, Hair ML. Detection of Superoxide Ions in Non-Aqueous Media - Generation by Photolysis of Pigment Dispersions. J Phys Chem. 1978; 82:1397–1399.
30. Merlin JL, Azzi S, Lignon D, Ramacci C, Zeghari N, Guillemin F. Mtt Assays Allow Quick and Reliable Measurement of the Response of Human Tumor-Cells to Photodynamic Therapy. European Journal of Cancer. 1992; 28A:1452–1458. [PubMed: 1387543]
31. Rosen GM, Beselman A, Tsai P, Pou S, Mailer C, Ichikawa K, Robinson BH, Nielsen R, Halpern HJ, MacKerell AD. Influence of conformation on the EPR spectrum of 5,5-dimethyl-1-hydroperoxy-1-pyrrolidinyloxyl: A spin trapped adduct of superoxide. J Org Chem. 2004; 69:1321–1330. [PubMed: 14961686]
32. Pieta P, Petr A, Kutner W, Dunsch L. In situ ESR spectroscopic evidence of the spin-trapped superoxide radical, O-2(center dot-), electrochemically generated in DMSO at room temperature. Electrochim Acta. 2008; 53:3412–3415.
33. Kavarnos GJ, Turro NJ. Photosensitization by Reversible Electron-Transfer - Theories, Experimental-Evidence, and Examples. Chem Rev. 1986; 86:401–449.
34. Worthington P, Hambright P, Williams RFX, Reid J, Burnham C, Shamim A, Turay J, Bell DM, Kirkland R, Little RG, Dattagupta N, Eisner U. Reduction Potentials of 75 Free Base Porphyrin Molecules - Reactivity Correlations and the Prediction of Potentials. J Inorg Biochem. 1980; 12:281–291.
35. Kanoufi F, Zu YB, Bard AJ. Homogeneous oxidation of trialkylamines by metal complexes and its impact on electrogenerated chemiluminescence in the trialkylamine/Ru(bpy)(3)(2+) system. J Phys Chem B. 2001; 105:210–216.

36. Jiang XJ, Lo PC, Yeung SL, Fong WP, Ng DKP. A pH-responsive fluorescence probe and photosensitiser based on a tetraamino silicon(IV) phthalocyanine. Chem Commun. 2010; 46:3188–3190.

37. Zhao H, Joseph J, Fales HM, Sokoloski EA, Levine RL, Vasquez-Vivar J, Kalyanaraman B. Detection and characterization of the product of hydroethidine and intracellular superoxide by HPLC and limitations of fluorescence. Proc Natl Acad Sci U S A. 2005; 102:5727–5732. [PubMed: 15824309]

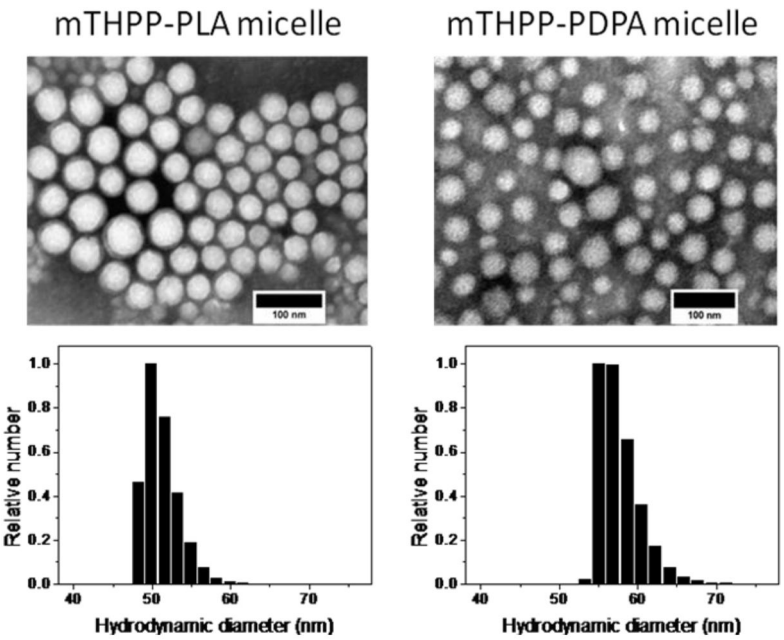

Figure 1.
Transmission electron microscopy (TEM) images of mTHPP-loaded micelles counter-stained with 2% phosphotungstic acid. The scale bars are 100 nm. Histograms depict hydrodynamic diameter distributions of mTHPP-loaded micelles by dynamic light scattering (DLS).

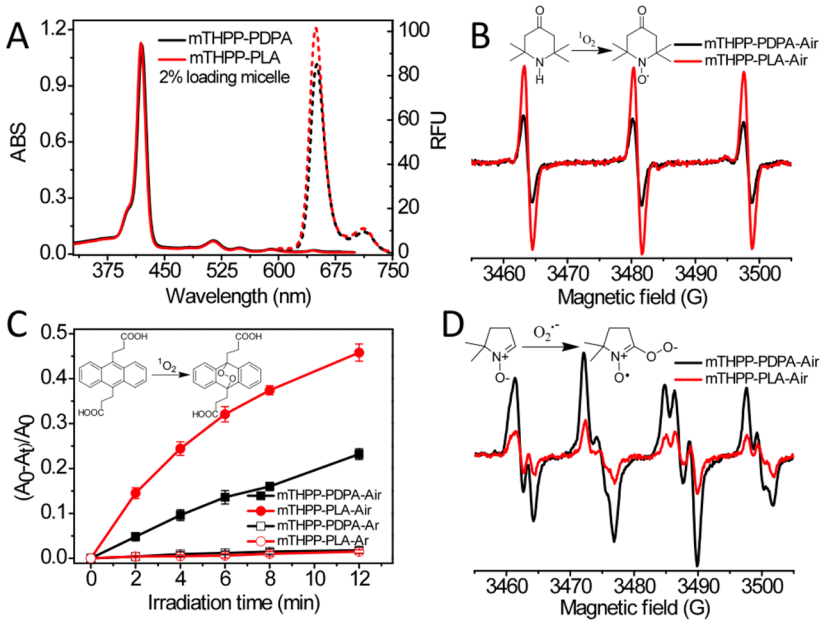

Figure 2.

(A) Absorption (solid line) and fluorescence spectra (dashed line) of mTHPP-PLA (red) and mTHPP-PDPA micelles (black) in H_2O. Micelle concentration = 100 g/ml, λ_{ex} = 420 nm. (B) Photoinduced ESR spectra of TEMP-$^1O_2$ adduct produced from irradiation of mTHPP micelles in H_2O (λ = 532 nm) for 400 seconds. (C) ADPA consumption by reaction with $^1O_2$ over time in H_2O containing 200 μg/ml mTHPP micelles irradiated with 532 nm laser light in air and argon saturated solutions. (D) ESR spectra of DMPO-superoxide radical adduct produced from irradiation of mTHPP with PEG-PLA or PEG-PDPA in DMSO with 532 nm laser exposure for 120 seconds. ESR spectral parameter settings: microwave power, 10 mW; modulation amplitude, 1.0 G; receiver gain, 1×10^5.

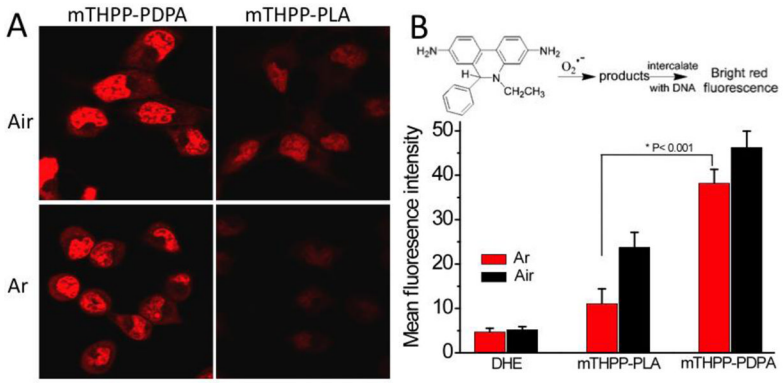

Figure 3.

(A) Confocal laser scanning microscopy images of H2009 lung cancer cells after incubation with 150 μg/ml mTHPP micelles for 2 hrs, followed by incubation with DHE for 30 mins in air or argon-saturated PBS, then irradiated with 532 nm laser light at 20 mw/cm^2 for 4 mins. (B) Average fluorescence intensity from 10 cells calculated by ImageJ for different treatment groups. H2009 cells without mTHPP micelle treatment, but incubated with DHE were used as the control (DHE).

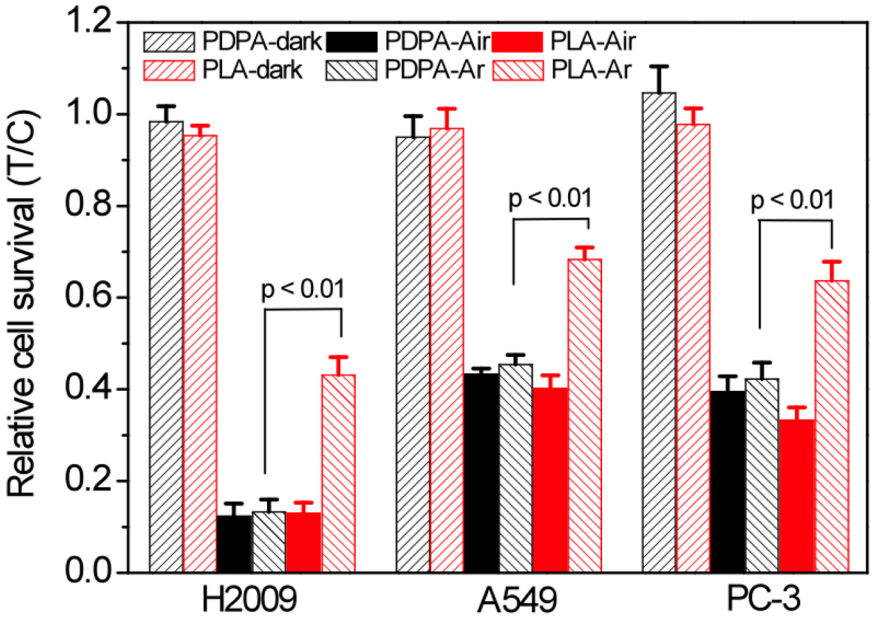

Figure 4.

Relative survival of different cancer cells irradiated with 12 J/cm^2 (power density 20 mW/cm^2) of 532 nm light in atmospheres of air and argon. Micelle concentration: 200 μg/ml. Incubation time: 2 h. Values represent treat/control (T/C) ± standard deviation (N = 6).

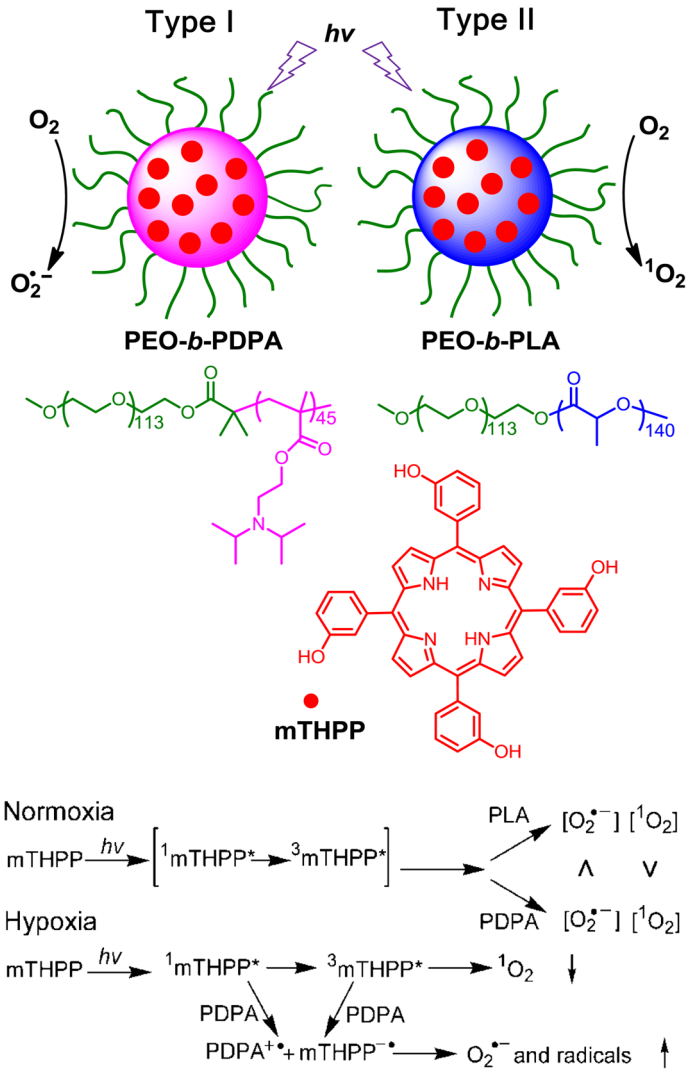

Scheme 1.

Modulation of photoactivation mechanism of a model photosensitizer, mTHPP, by the micelle microenvironment at normoxic (~50 mmHg O_2) and hypoxic (<20 mmHg) conditions. Electron-rich PDPA micelles led to increased type I reactions producing superoxide radical anions, while electron-deficient PLA micelles generated singlet oxygen as predominant species by type II reactions.

Table 1

Comparison of the physical properties of free mTHPP and mTHPP-PLA and mTHPP-PDPA micelles.

Samples	Loading density (%)[a]	Diameter (nm)[b]	ξ (mV)	Soret band (nm)	Q-bands (nm)	Emission (nm) (Φ_f)	E (V) vs SCE	Φ_Δ[c]	$\Phi_{O_2^{\bullet-}}$[d]
Free mTHPP[e]	–	–	–	415	512,546,589,643	650 (0.12)	−0.98[g]	–	–
Free mTHPP[f]	–	–	–	428	523,557,590,645	642 (<0.01)		–	–
PEG-PLA	–	41 ± 5	−6.9 ± 4.5	–	–	–		–	–
PEG-PDPA	–	50 ± 6	2.0 ± 3.8	–	–	–	0.65[h]	–	–
mTHPP-PLA	1.8 ± 0.5	49 ± 6	−8.1 ± 7.5	419	514,549,589, 646	649 (0.11)		1	1
mTHPP-PDPA	1.9 ± 0.4	57 ± 6	1.6 ± 5.9	420	514,549,590,647	649 (0.08)		0.46	3.9

[a] mTHPP loading density was measured as the weight of mTHPP over that of total micelles.

[b] By dynamic light scattering.

[c] Relative $^1O_2$ yields that were normalized to that of 2% mTHPP PEG-PLA micelles in H_2O using ADPA as a $^1O_2$ probe.

[d] Relative $O_2^{\bullet-}$ yields that were normalized to 2% mTHPP-PLA in DMSO using DMPO as a spin trap.

[e] In methanol.

[f] In phosphate buffer (PB).

[g] the reduction potential (Epa) of mTHPP in DMF.

[h] the oxidation potential (Epc) of PEG-PDPA in DMF.